## III.D. FOURIER IMAGE PROCESSING TECHNIQUES

### III.D.1. Optical Diffraction

Optical diffraction is the simplest and most widely practiced Fourier image processing technique, and is **usually** the initial step in many image processing studies. The main advantage of this technique is that it provides an objective way to assess and reveal periodic structural information. Klug and Berger (1964) were the first to use an optical bench to examine diffraction patterns of electron micrographs and thereby objectively analyze structural information in images of biological specimens.

#### a. Forming the diffraction pattern

Optical diffraction patterns are easily produced from selected (masked) regions of micrographs. A simple optical bench consists of a laser, to produce a parallel, monochromatic beam, which illuminates a specific area of the micrograph, and a (diffraction) lens to focus the Fraunhofer diffraction pattern in the back focal plane of the lens. The pattern may be viewed directly, but cautiously to avoid focusing the bright, central spot formed from the unscattered rays on the retina, or it may be recorded on a standard photographic emulsion.

#### b. Experimental apparatus: the optical diffractometer

There are several diffractometer designs, which fall into one of two basic classes depending on whether the optical path is straight (**linear diffractometer**: Fig.III.58) or bent by use of optically flat mirrors (**folded diffractometer**: Figs.III.59 and 60). The type of diffractometer one chooses to use depends, in part, on the intended use of the apparatus. The folded design is usually preferred for rapid screening of a large number of micrographs when image quality and specimen preservation need to be assessed in order to select images for subsequent optical (Sec. III.D.2) or digital (Sec. III.D.3) filtering operations. For high quality optical reconstruction work, the linear design is generally preferred since there are fewer optical components, and thus fewer aberrations.

A diffractometer of reasonable quality, suitable for simple experiments such as screening images or detecting and locating periodicities, can be built or purchased for a few thousand dollars or less. More expensive designs ($10,000 or more) are usually easier to use and align, and produce high quality diffraction patterns and reconstruction images. A quality diffractometer usually includes an image reconstruction system (with a high-quality, corrected, doublet lens), a pinhole spatial filtering system to remove noise in the illumination beam, a moderate-to-high power laser (1-50 mWatt), high-quality, high-reflectance mirrors (if the optical path is folded), fully adjustable, precision holders for all components, and an image and diffraction pattern recording system.

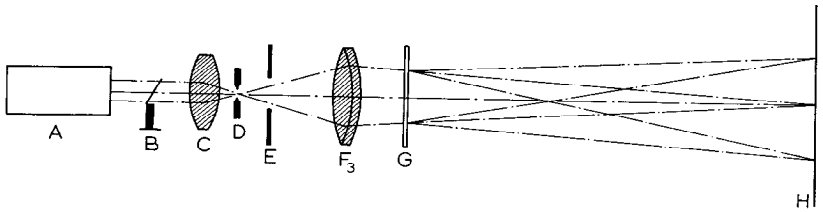


Fig.III.59. Simple optical diffractometer. The diagram shows the arrangement of the components used to construct a simple optical diffractometer. A. laser; B, shutter; C, beam expanding lens; D, pinhole; E, adjustable diaphragm; F3, diffraction lens; G, electron micrograph; and H, viewing screen or camera. (From Horne and Markham, p.336)

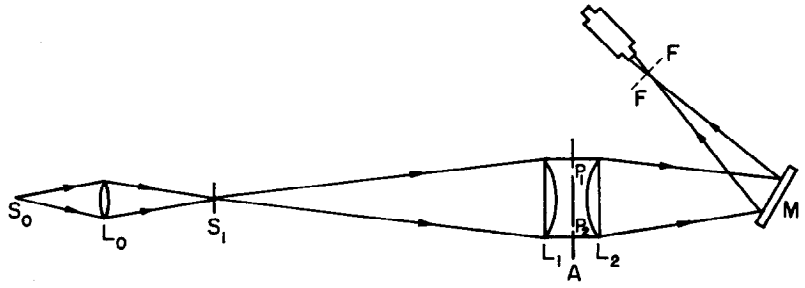


Fig.III.60. Schematic diagram of an optical diffractometer. (From Thompson (Lipson), p.48)

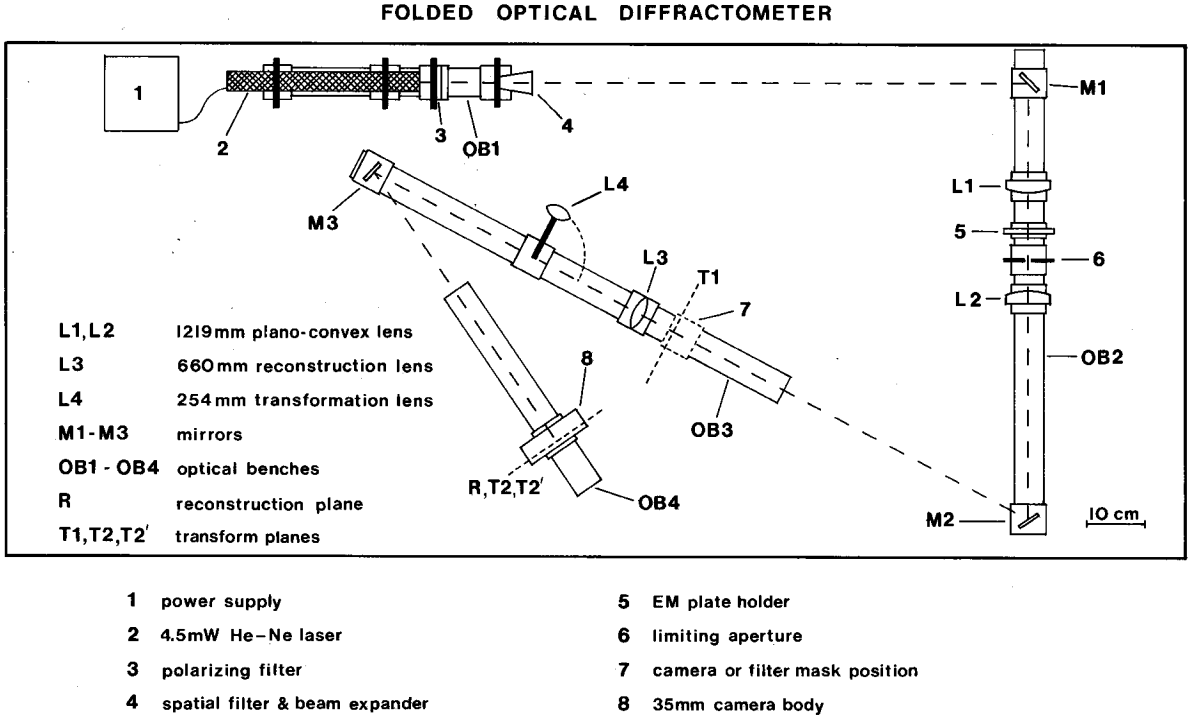


Fig.III.61. Diagram of the UCLA folded optical diffractometer, built in 1972.

Many laboratories prefer to construct their own diffractometer with specifications dictated by the intended use of the instrument. For example, if most of the image reconstruction work is to be performed on a computer, a simple and inexpensive linear diffractometer for surveying images will suffice. The use of liquid gates, in which micrographs are submerged in oil to iron out in homogeneities in the micrograph emulsion (and glass or gelatin backing), produce diffraction patterns in which Friedel symmetry is nearly perfectly preserved (Table 1.I.C.2.e, Baker, 1981). However, such extreme measures prove inconvenient and, in any event, digital processing systems are both fast and reliable and are usually preferred over high-quality optical processing systems.

Details of the design, operation, components, alignment, and calibration of optical diffractometers can be found in several references (Horne and Markham, 1972; Mulvey, 1973; Johansen, 1975; Erickson, *et al.*, 1978; Baker, 1981). The optical diffractometer, much like the electron microscope, needs to be carefully aligned and calibrated to perform optimally.

### c. Applications of optical diffraction

Optical diffraction provides useful information about the geometrical arrangement of subunits in the specimen. Such structural detail often cannot be discerned by simple, visual inspection of the original micrograph. For example, the presence of rotational screw axes or pseudo-symmetries

may go undetected without the information provided by the optical diffraction pattern. These types of structural information are determined by correctly indexing the pattern, that is, defining a lattice (or lattices for multilayered or helical particles) that accurately defines the location of all diffraction spots.

Indexing is an essential step for correct application of optical or digital filtering, or 3D reconstruction techniques (Sec. III.D.2). With an exception for some helical and multilayered particles, the indexing of OD patterns from most planar specimens is quite straightforward. Articles by Finch, Klug and Nermut (1967), Moody (1967), Kiselev and Klug (1969), Mikhailov and Belyaeva (1971), DeRosier and Klug (1972), Lake (1972b), Leonard, Kleindschmidt and Lake (1973), and Unwin and Taddei (1977) give excellent, examples of pattern indexing (these and additional examples are cited in Table 1.I.D.8, Baker, 1981). Misell's book (1978; pp.106-122) devotes an entire section to theoretical and practical problems of indexing. Artifacts in optical diffraction patterns can make indexing difficult (Table 1.I.E, Baker, 1981). The characteristic and often prominent "cross" observed in many optical diffraction patterns is mainly a consequence of strong diffraction caused by the edges of the mask used to select a region of interest in the micrograph. This feature is regarded as "noise" in the pattern and thus, should not influence the selection of a consistent indexing scheme. Fig.III.62 shows a typical example of an optical diffraction pattern recorded from an image of a negatively stained 2D crystal of catalase. Other examples will be shown in class.

Several applications of optical diffraction include:

- Accurate measurement of lattice parameters (unit cell dimensions). (Fig.III.62)
- Detection of rotational and translational symmetry elements. (Fig.III.62)
- Determine relative orientation of multilayered specimens (*e.g.* stacked 2D sheets or opposite sides of two-sided structures).
- Detect and measure specimen preservation (distortions, overall resolution, radiation damage) for selecting best images for further image analysis.
- Assess short/long range order in periodic specimens. (Fig.III.63)
- Identification of signal vs. noise in images. (Fig.III.62)
- Ability to examine specific small areas. (Figs.III.62, 64-66)
- Determine electron optical conditions, i.e. contrast transfer function (focus, drift, astigmatism, etc.) at time micrograph was recorded. (Figs.III.62, 64-66)
- Determine the hand of 3D structures (from metal-shadowed or tilted specimens).
- Superb device for teaching principles of diffraction, symmetry, and Fourier transforms.

Optical diffraction techniques have been successfully employed in fields outside electron microscopy, for example, in the study of small-molecule crystal structures. In fact, pioneers of crystallography made much of the original development of diffractometers. W. L. Bragg (1939) designed the first optical diffractometer, calling it a "new type of X-ray microscope". Several crystallographers used optical diffraction methods as an aid in solving small molecule crystal structures. By comparing diffraction patterns produced by models of the crystal structure (using various size holes punched in sheets of metal at predicted positions to represent atoms) with the experimentally recorded x-ray diffraction patterns, it was often possible to rule out incorrect structures and thereby verify or solve a crystal structure.

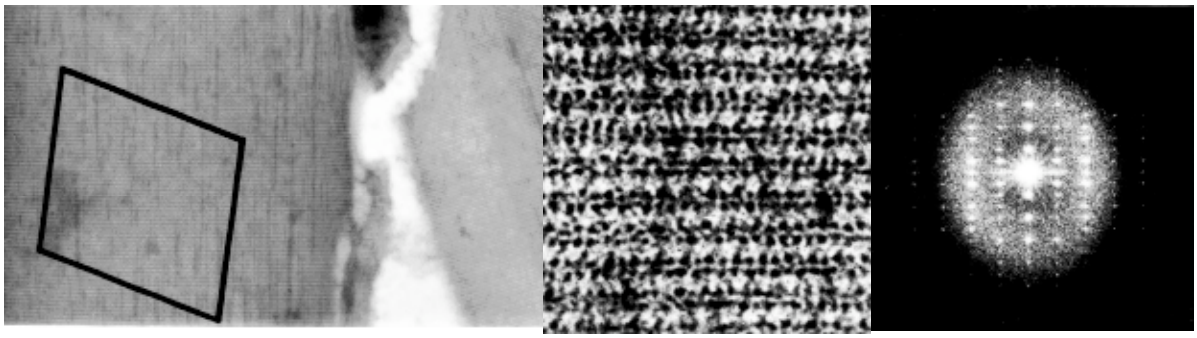

Fig.III.62. (Left) Low magnification micrograph of negatively stained bovine liver catalase. (Right) High magnification view of small portion of same crystal. (Right) Optical diffraction pattern recorded from the area outlined in the low magnification image.

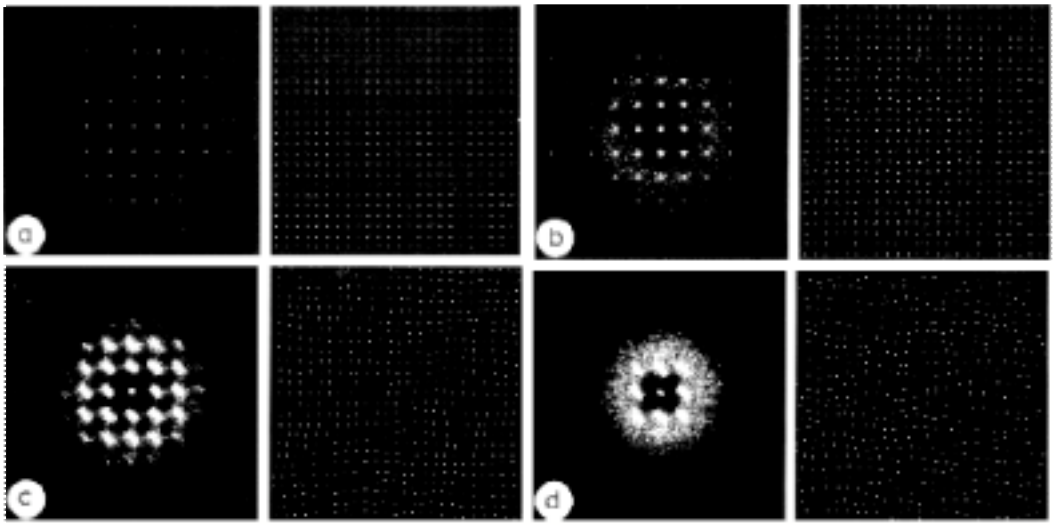


Fig.III.63. The effect of lattice disorder on the diffraction pattern. (a) Ordered lattice. (b) Vertical disorder of ±10%. (c) Two-dimensional disorder of ±10%. (d) Two-dimensional disorder of ±25%. (From Misell, 1978, p.72)

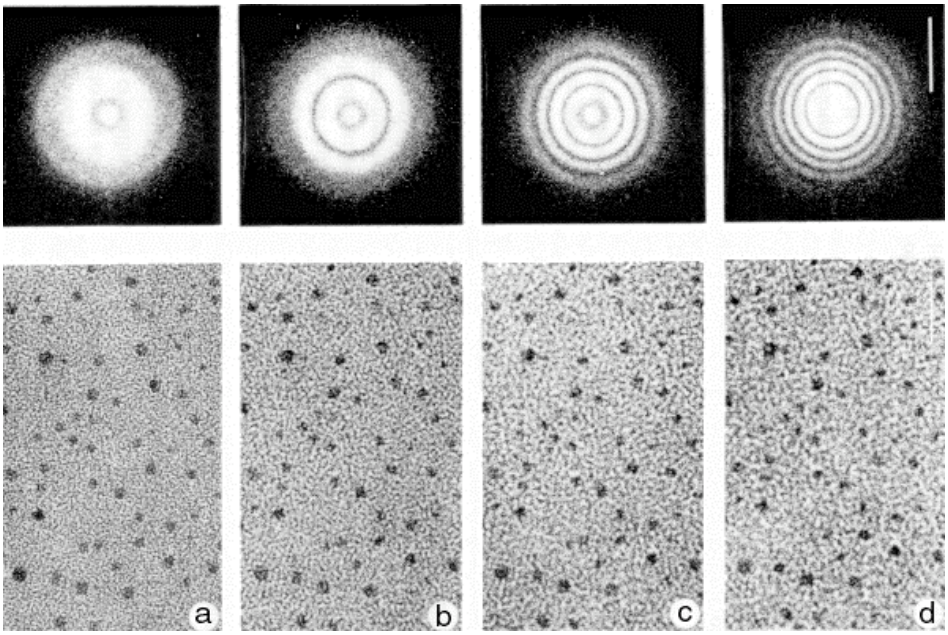


Fig.III.64. Focus series of thin carbon film. The black dots are gold atoms added to assist in focusing. The optical diffraction patterns above each image indicate (a) optimum defocus, (b) 150 nm underfocus, (c) 210 nm underfocus, (d) 250 nm underfocus. Image bar = 10nm. Diffraction bar = 3.0 $nm^{-1}$. (From Misell, 1978, p.60)

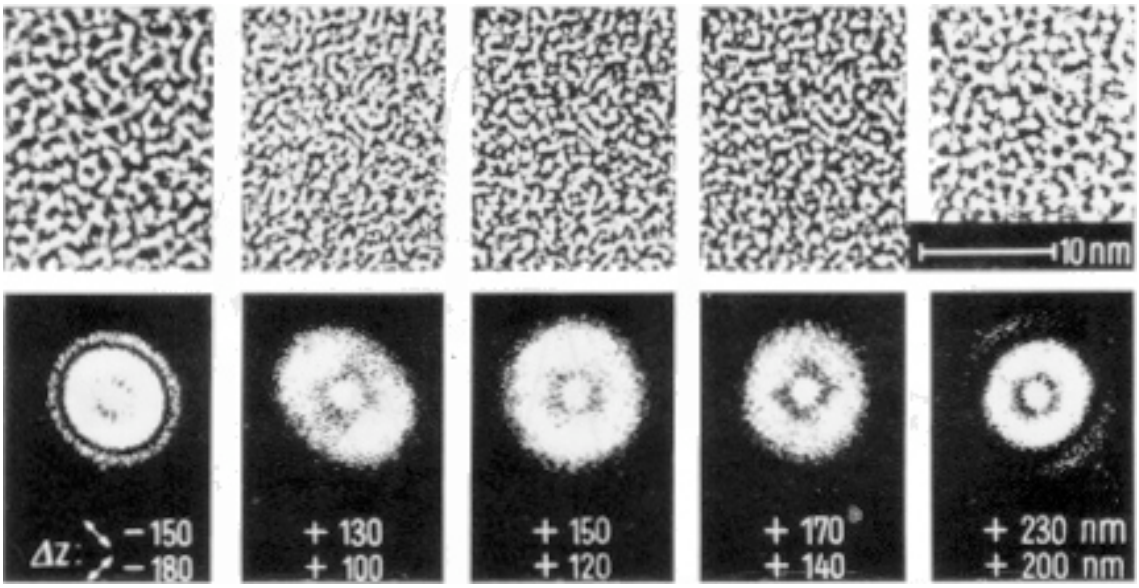


Fig.III.65. Micrographs and optical transforms of a carbon film, showing the effect of axial astigmatism and the determination of its direction. (From Misell, 1978, p.64)

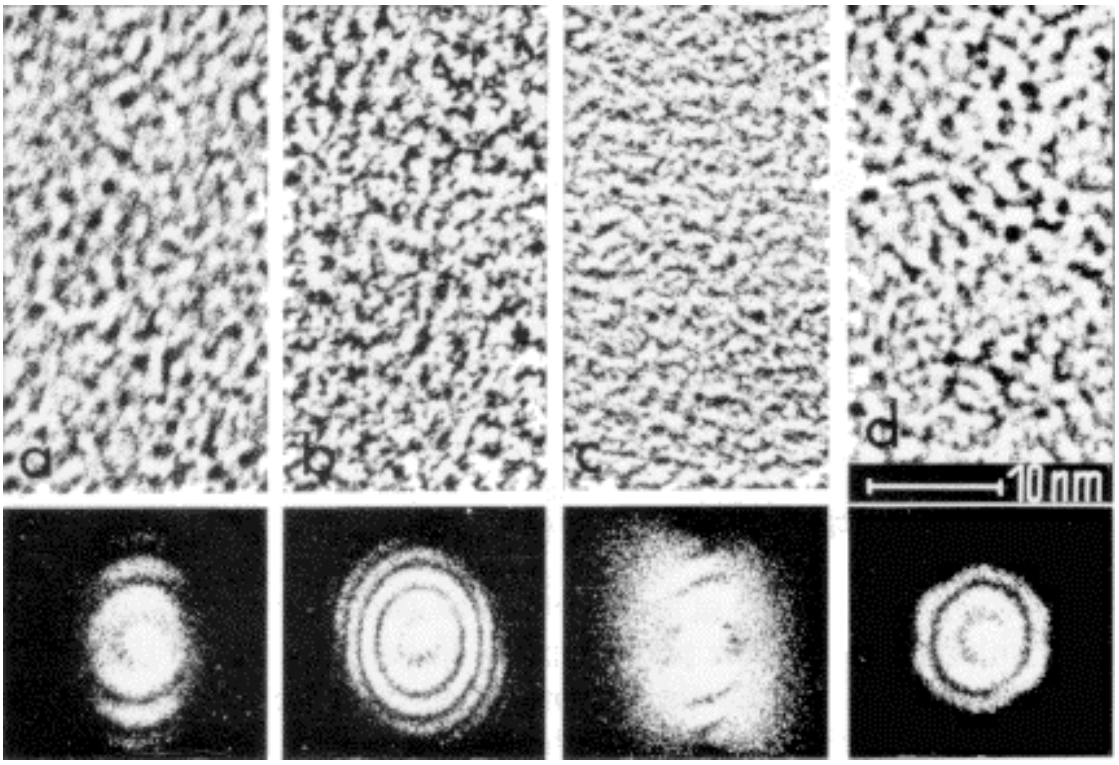


Fig.III.66. Images of a carbon film (top row) and corresponding optical transforms (bottom row), showing different image defects: (a) specimen drift, (b) miscentered objective aperture, (c and d) electrical charging of the objective aperture as a result of contamination, for example. (From Misell, 1978, p.65)

## III.D.2. Optical Filtering

Optical filtering, independently introduced by Klug and DeRosier (1966) and Bancroft, Hills and Markham (1967), is only suitable for the study of periodic specimens with translational symmetry. The main advantage of this method is it provides a simple way to remove the contributions from noise in micrographs and thereby reveal clearer images of specimen structure. In addition, it is a powerful method for separating Moiré images of multilayered specimens. Other applications are outlined Table 1.II.B of Baker (1981).

The review by Erickson, Voter, and Leonard (1978) and articles by Klug and DeRosier (1966) and Fraser and Millward (1970) give excellent introductions to the theory and techniques of optical filtration. The basic principle of the technique is straightforward, but, in practice, the method can easily lead to erroneous results. This is especially true for uninformed novices who are likely to be unaware of the types of artifacts that can occur.

### a. Indexing the diffraction pattern

The first, and **most important step** in an optical filtering experiment is to **correctly index** the optical diffraction pattern of the specimen. A pattern is considered successfully indexed if it is possible to distinguish between spots arising from noise (aperiodic image details) and those attributed to the periodic nature of the specimen. Although it is unnecessary to attempt to identify all the noise components in the unprocessed image, a correct filtration experiment requires knowledge of how noise and signal components are distinguished. For most crystalline specimens, the diffraction pattern is a lattice of bright spots (reflections) against a weaker background of noise (Figs.III.62, 67-68). Noises, or aperiodicities in the image, produce spots in all parts of the pattern. Note that **noise (periodic noise), which** appears at or close to the lattice points of the diffraction pattern, **CANNOT be removed** by filtering. Systematic specimen flattening or staining artifacts are examples of situations that produce periodic-type noise. Other major sources of noise are listed in Sec. III.B (p.178).

If the diffraction pattern is difficult to index, an incorrect lattice may have been identified (*e.g.* because a super lattice has been missed). Occasionally, strong, non-indexible spots may be attributed to multiple scattering (Table 1.I.D.7, Baker, 1981) or they might arise from strong, aperiodic features in the specimen. The temptation may be to ignore images with non-indexible patterns, but difficulties with indexing often clearly indicate that important structural information has been overlooked. Novices of image processing will benefit from study of the indexing examples in Misell's book (1978; pp.106-122) and cited in Table 1.I.D.8 of Baker (1981). Figures III.64-67 illustrate some aspects of the indexing of OD patterns.

### b. Filtering procedure

Once the diffraction spots are found to be consistent with a given lattice, a filter mask is designed with holes positioned to allow unobstructed passage of the diffraction spots at the lattice points (or lattice lines for helical particles). The mask is accurately positioned in the diffraction plane of the optical diffractometer so all spots at the lattice points are allowed through (Fig.III.73). Opaque regions of the mask block out most of the noise in the diffraction pattern arising from non-periodic image features. A reconstruction lens, placed behind the mask, refocuses the unobstructed rays and forms a filtered image. An **unfiltered** image is formed if the mask is removed. Optical reconstruction illustrates the Abbe double-diffraction phenomena of image formation (Sec. III.C.6.d): the diffraction pattern of the micrograph is formed in the first stage (forward transformation), and, in the second stage the reconstruction lens acts to rediffract the diffracted rays (back- or reverse transformation) to form an image (filtered or unfiltered). Thus, a filtered or unfiltered image is the result of rediffraction of the masked or unmasked diffraction pattern of the object (micrograph).

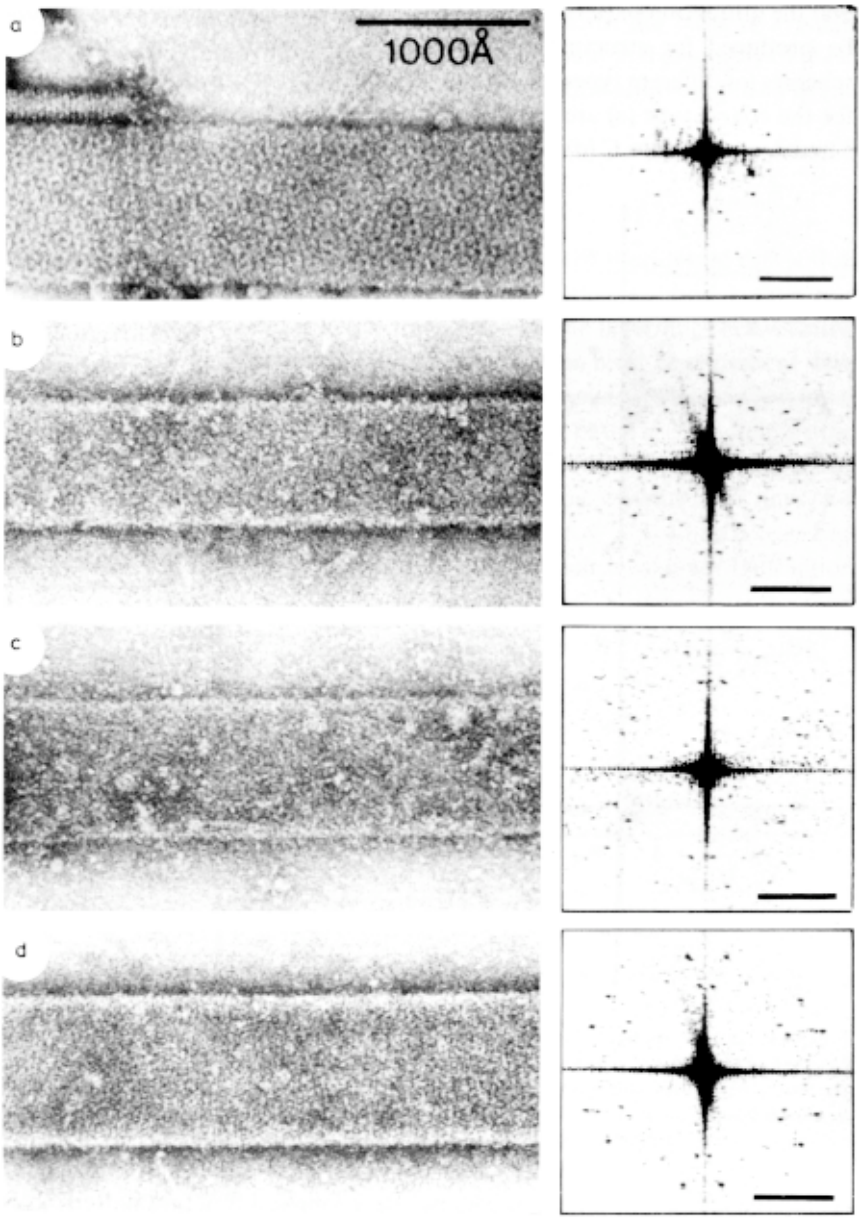


Fig.III.67. Electron micrographs and optical diffraction patterns of four different kinds of T-even polyhead. All specimens were negatively stained with 2% NaPT. (a) Coarse polyhead. (b) A-type polyhead. (c) B-type polyhead. (d) C-type polyhead. Differences in the OD patterns reflect differences (that can't be seen by naked eye) in the 'crystal' lattice structures. (From Steven *et al.*, 1976a, p.192)

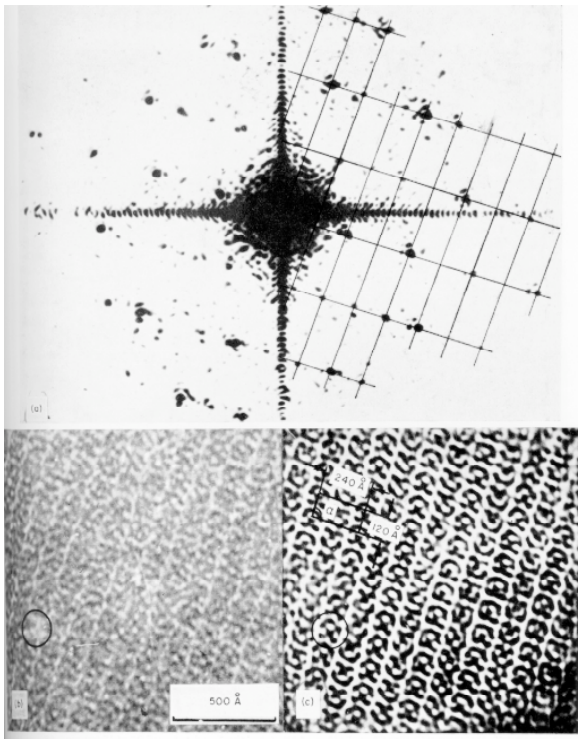


Fig.III.68. Optical diffraction of a portion of a plane layer of phosphorylase b particles and optical filtering of the image. (a) OD pattern (right hand part is indexed on the reciprocal lattice). (b) Portion of a 2D crystal before filtering experiment (stain here is white and protein is black). The particle in the circle is missing. (c) Filtered image. The missing particle shows up as a result of the averaging action of filtering. The unit cell shown on the image corresponds to the reciprocal lattice of (a). (From Kiselev *et al.*, 1971, Plate III)

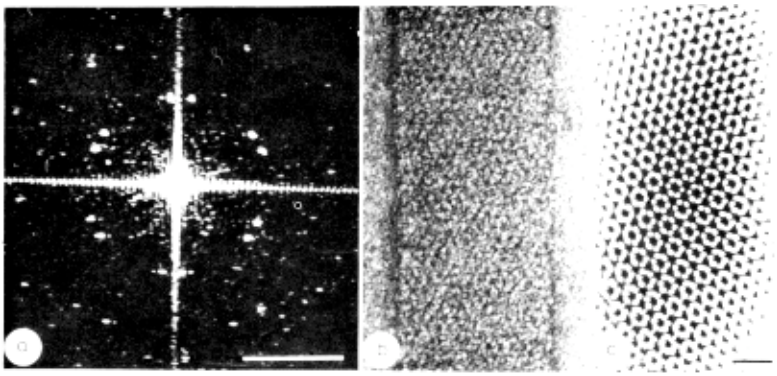

Fig.III.69. (a) Optical transform. (b) Micrograph of negatively stained bacteriophage T4 polyhead (coarse). (c) One-sided optical reconstruction of the polyhead lattice. Image bar = 20 nm. Diffraction bar = 0.2nm$^{-1}$. (From Misell, 1978, p.116)

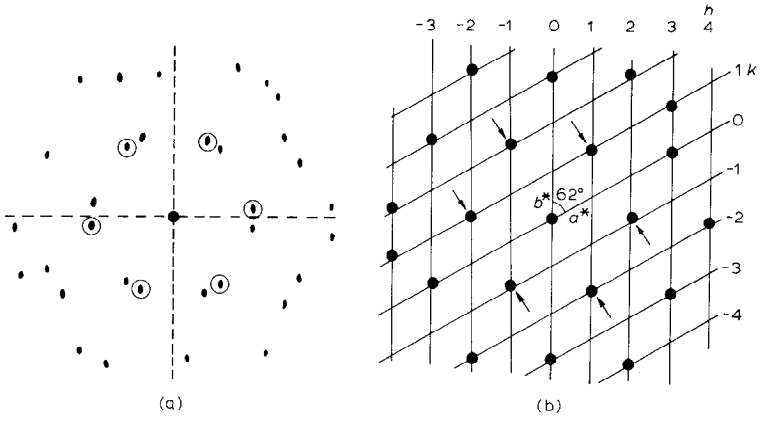


Fig.III.70. Reciprocal lattice for the coarse polyhead shown in Fig.III.69. The first order of the hexagonal lattice is missing. Note also that these schematic representations of the OD pattern (a) and one side of the reciprocal lattice (b) are rotated 90 degrees with respect to the OD pattern depicted in Fig.III.69. (a) Original OD pattern with spots from one-side ringed. (b) Reciprocal lattice drawn through the spots resulting from one-sided diffraction (arrowed). (*h,k*) define the diffraction order; *a** and *b** are the reciprocal lattice constants. *a** = *b** for a hexagonal lattice. (From Misell, 1978, p.116).

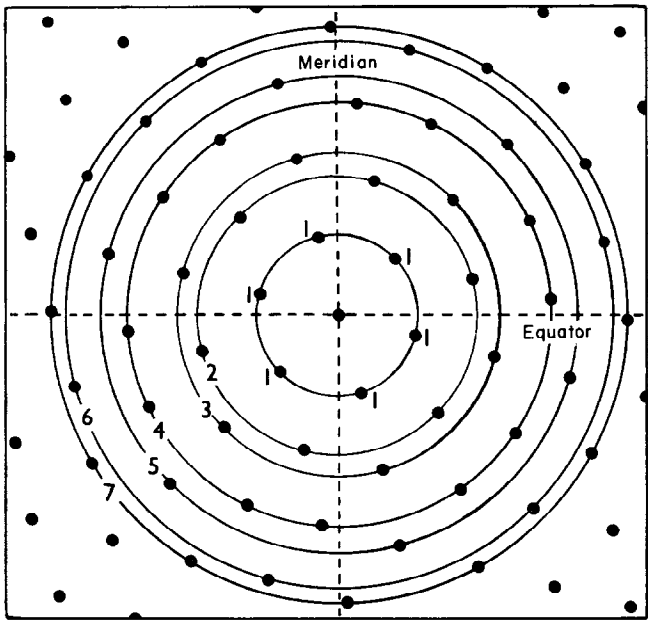


Fig.III.71. A capsomer with 6-fold symmetry convolved over a hexagonal lattice generates a diffraction pattern in which the Fourier transform of the capsomer is sampled on a hexagonal reciprocal lattice. The 6-fold symmetry of the capsomer is reflected in its Fourier transform in that, in the absence of noise, each diffraction spot is related to five other hexagonally conjugate spots. These sextets of equivalent spots lie on concentric circles which, in order of increasing radius we refer to as 1st, 2nd, 3rd, etc. orders, as shown in the schematic drawing. The radii of these circles bear fixed ratios to one another ($R_1$:$R_2$:$R_3$:$R_4$ etc. = 1:$\sqrt{3}$:2:$\sqrt{7}$ etc.). In practice, sources of electron micrograph noise, as well as departures from exact symmetry, comprise the equivalence of hexagonally conjugate spots, but indexation of the diffraction pattern is possible provided at least two orders are visible. (From Steven *et al.*, 1976a, p.194)

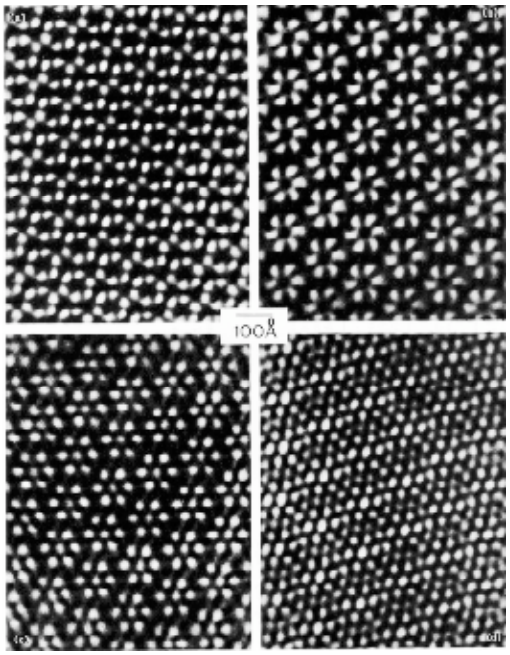


Fig.III.72. Optical filtrations of the four major classes of T4 polyhead as shown in Fig.III.67. Upper left: coarse polyhead. Upper right: A-type polyhead. Lower left: B-type polyhead. Lower right: C-type polyhead. (From Steven *et al.*, 1976a, p.200)

## c. Filtering apparatus

(Figs.III.73-75)

Filtration experiments are performed on an optical diffractometer equipped with a reconstruction lens (or lenses). The reconstruction system must be of high optical quality to minimize image distortions (*e.g.* phase errors due to spherical aberration). Camera lenses often make suitable reconstruction lenses, although they are usually expensive and not ideally designed for the purposes of the optical reconstruction experiment (camera lenses are generally designed for optimum transmission of light, not for flatness of field). A high quality, but inexpensive, corrected doublet, with a large usable aperture, can produce high resolution, reconstruction images.

Most image processing laboratories use a folded diffractometer (*e.g.* Fig.III.61) both for survey and reconstruction work, mainly because it is more convenient to operate compared with a linear-type apparatus. The main disadvantage of the folded design is that mirrors are required to bend the optical light path. Mirrors add extra optical surfaces, which collect dust or become scratched and thus can deteriorate the quality of the diffraction pattern or reconstruction image. Expensive, high-quality (high reflectance and optically flat) mirrors are recommended for optimum results. The quality of the optical bench is easily assessed by critically comparing an unfiltered reconstruction with the original image. The closer the match, the better the reconstruction system.

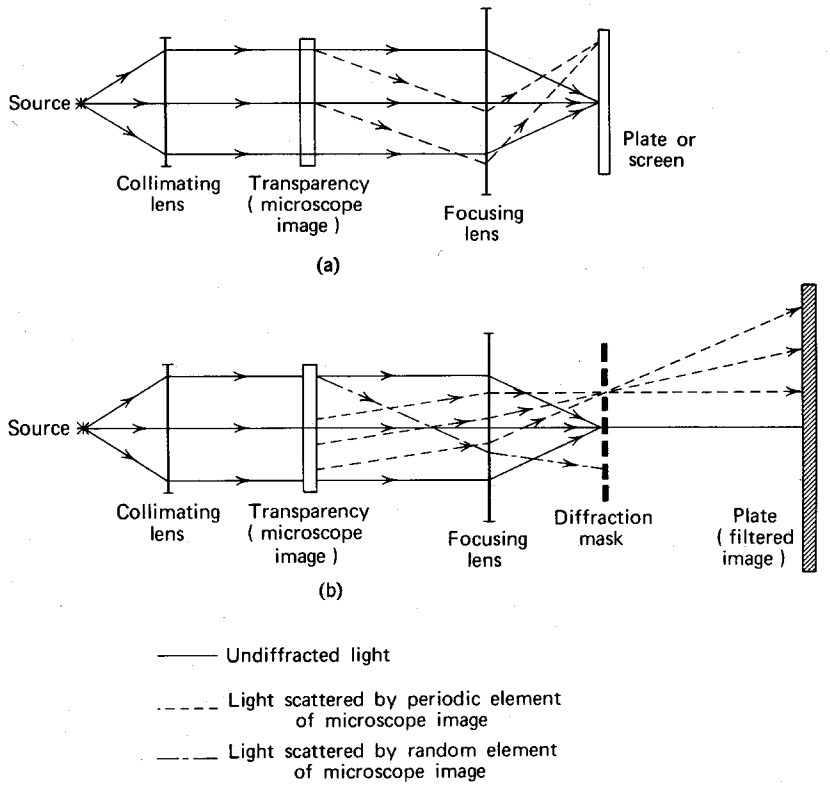


Fig.III.73. Optical filtering: (a) recording of diffraction pattern; (b) recording of the filtered image. Note that the paths of the dashed rays are inaccurate, because, for example, in (a) the ray that passes nearly through the center of the lens should bend only slightly (according to thin lens action, rays passing through the center of a thin lens will continue on a straight line. See Sec.I.A.4, pp.13-15). (From Slayter, p. 448)

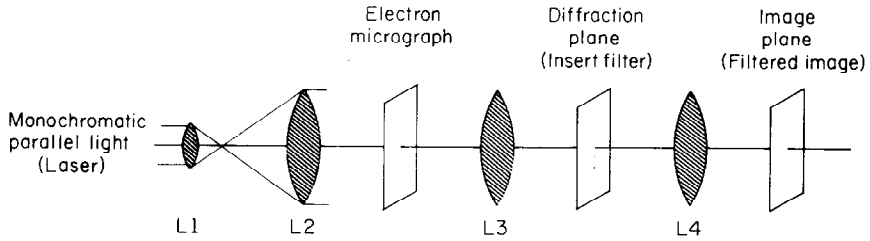


Fig.III.74. An optical system typically used to diffract and filter electron micrographs. (From Lake (Lipson), p. 63)

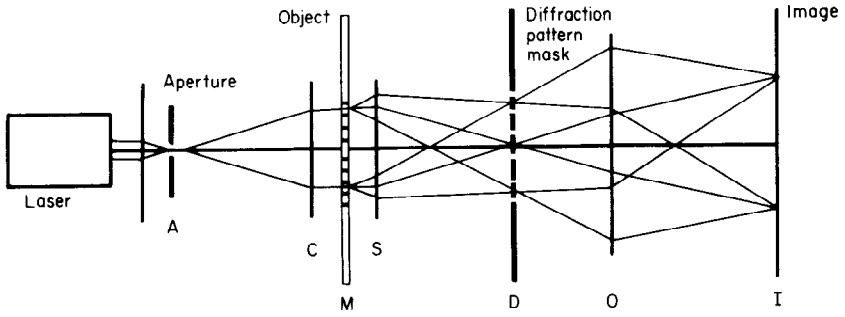


Fig.III.75. Schematic diagram of an optical diffractometer used to form a reconstructed image, I. C and S are the collimating and diffraction lenses, respectively and O is the reconstruction lens. (From Blundell and Johnson, p.110)

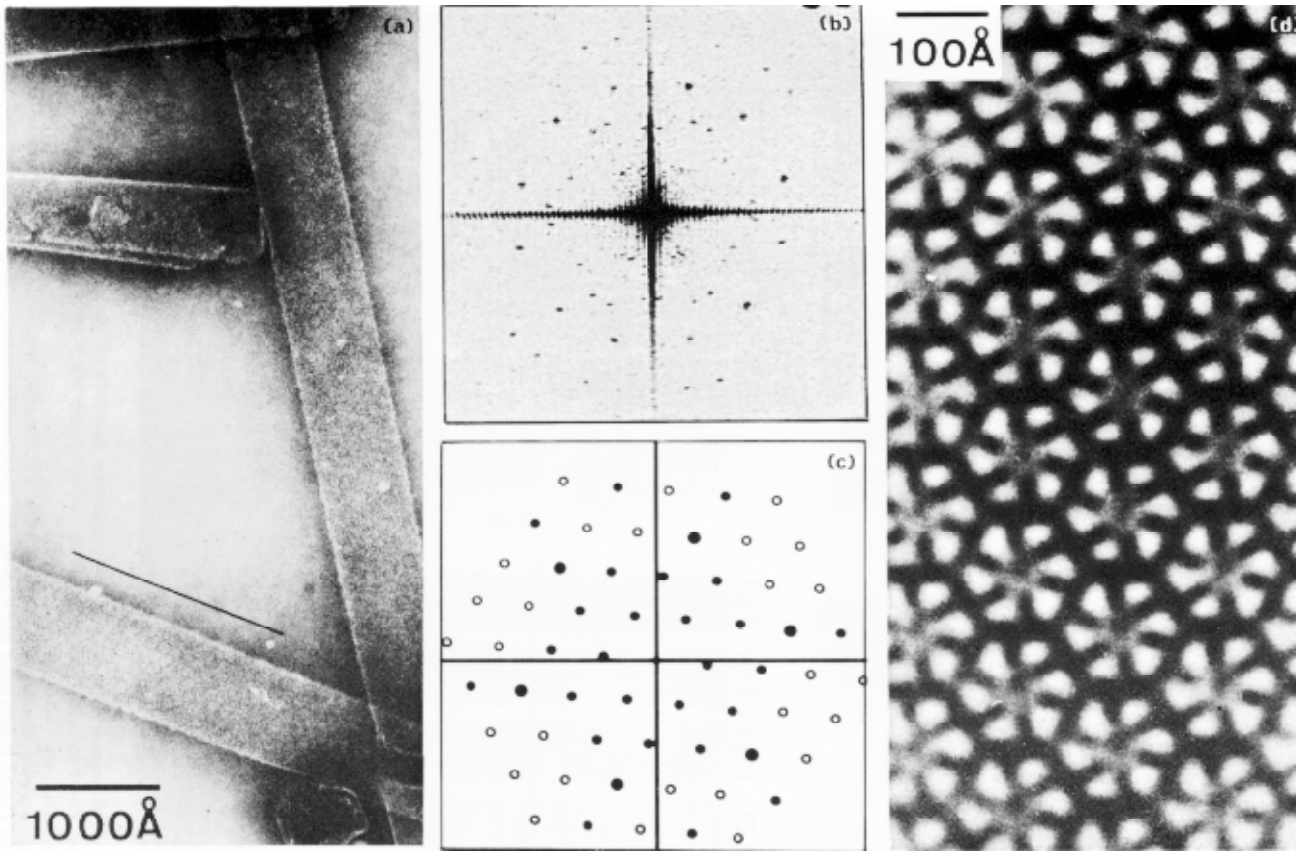


Fig.III.76. (a) Electron micrograph of AB-type T4 polyheads, negatively-stained with 2% NaPT. (b) OD pattern of the marked region of the polyhead. (c) Indexation of the reciprocal lattice of the diffraction pattern generated by one side of the flattened polyhead bilayer. Visible diffraction spots are shown with solid circles, invisible ones with empty circles. For orientation, the dominant spots of the 4th radial order are shown with larger full circles. The other diffraction spots can be obtained from the Indexation by reflection of the given lattice through the meridian (vertical axis). (d) Optical filtration of this polyhead. (From Steven *et al.*, 1976a, p.205)

### d. Design of filter masks

Once a consistent indexing scheme is established, the design and fabrication of the filter mask (Table 1.II.E, Baker, 1981) usually constitute the rate limiting steps in a filtration experiment. Etching procedures are used to produce precise masks: but, more tedious and demanding manufacturing skills are required compared to those for preparing masks by punching or drilling holes. Erickson, Voter and Leonard (1978) describe a simple method for producing suitable masks within minutes. Their method has the additional advantage of using the original, recorded pattern as a template.

### e. Image averaging

Optical filtering reduces image noise by averaging neighboring, periodically repeated units in the array. As the size of holes in the filter mask is reduced, more noise in the diffraction pattern is removed and the extent of local averaging increases (Figs.III.77-79). That is, the image of a given unit in the array is averaged with more of its neighbors. If holes are made smaller than the diffraction spots, the signal-to-noise ratio may decrease (Table 1.II.F.1.d, Baker, 1981).

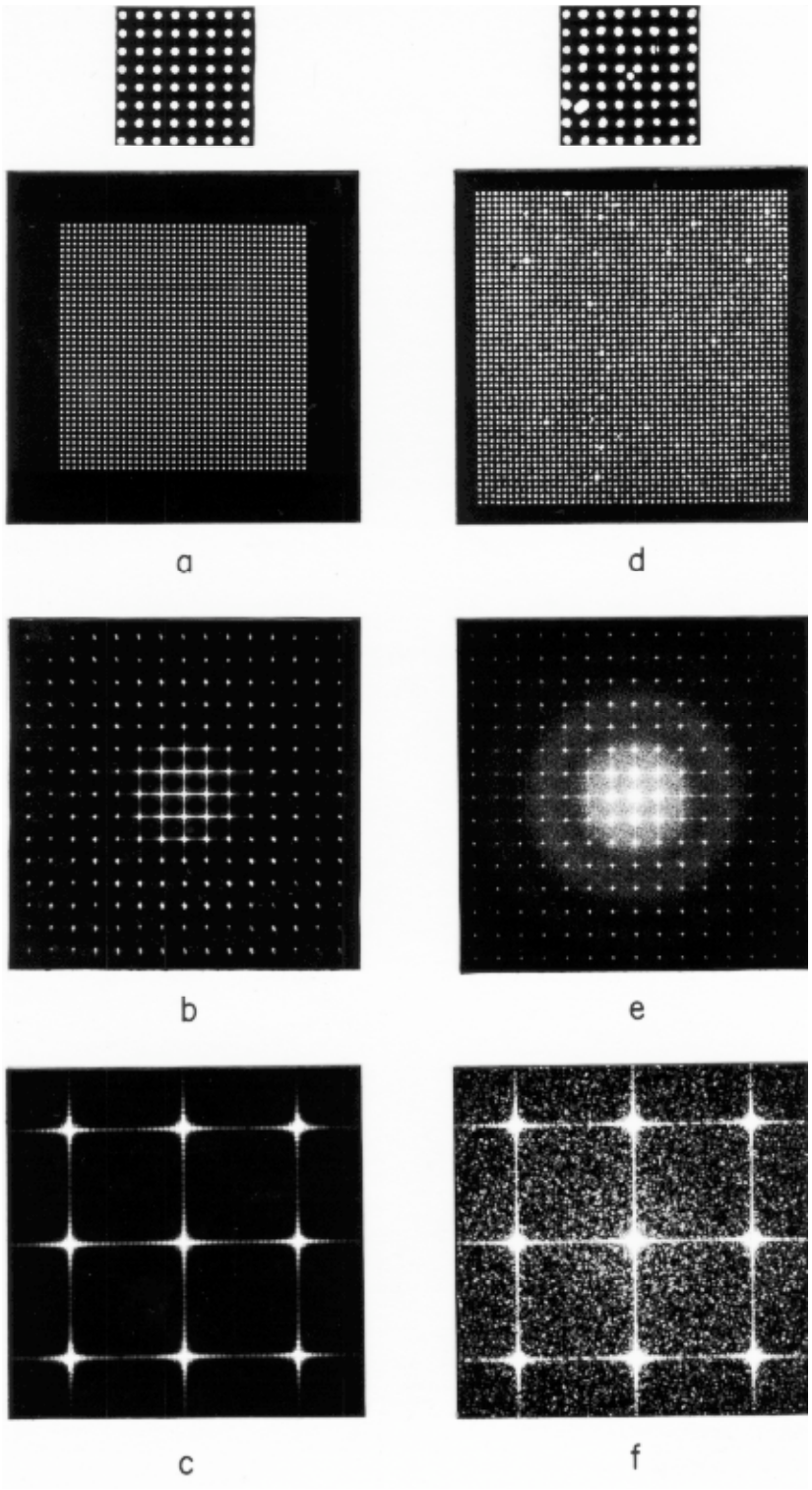


Fig.III.77. Optical filtering demonstration, Part 1. (a) 40 by 40 array of 'perfect' circular holes representing an idealized model of a crystal structure. A magnified portion appears directly above the complete array. The diffracting object is a copper foil with holes etched in it. (b) The OD pattern of (a). Note that the transform exists only at discrete lattice points (reciprocal lattice) except for the subsidiary maxima, which are shown more clearly in the enlarged view (c). Because (a) is the convolution of a circular hole with a 40 by 40 lattice of points, (b) is the transform of a single hole (Airy function) multiplied (or sampled) by a lattice which is the reciprocal of the lattice of (a). (c) Enlarged central region of (b) showing the subsidiary maxima between lattice points. The subsidiary maxima contain information about the overall shape of the diffracting object. If n is the number of repeating units in a given direction, then the number of subsidiary maxima along the same direction in the transform is n-2. Thus, by counting the number (38 in this example) of maxima between two lattice points in (c), the number of repeating units (40) can be determined without seeing the object. (d) 50 by 50 array of imperfectly shaped holes representing a distorted crystal structure. The magnified region (above) also shows an extra hole, which does not belong to the rest of the lattice. (e) Optical transform of (d). A large portion of the diffracted light falls between the lattice points, indicating the presence of aperiodic information in the object (d). (f) Enlarged central region of (e).

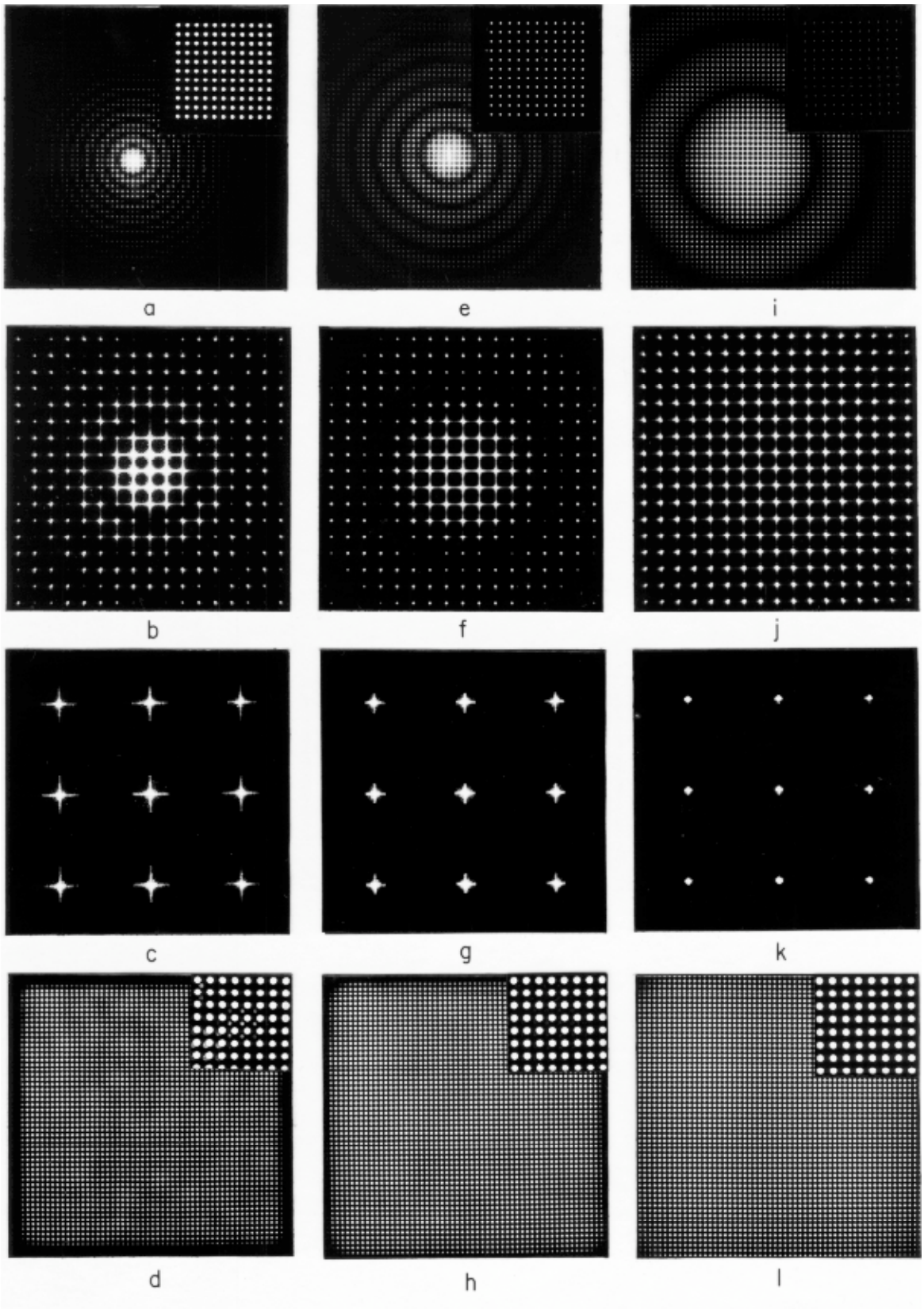


Fig.III.78. Optical filtering demonstration, Part 2. (a,e,i) Filtering masks (insets) and their transforms. The masks are identical 11 by 11 arrays except for the size of the holes. $d_a*/a^*$ = 0.43, 0.20, and 0.10 for the masks represented in (a), (e), and (i). The masks are designed to filter the central 11 by 11 array of the transform shown in Flg.III.77e. All

three mask transforms have the same lattice parameters (which must be identical with the object lattice), but they are multiplied by the transform of the different size holes in each case. As the mask hole gets smaller, the area of the central maximum of the hole transform (Airy function) increases. The mask transform is the function that the object (Fig.III.77d) is convoluted with, thus the size of the central maximum is the area of local averaging in the filtered reconstructions (d,h,l). (b,f,j) Enlarged views of (a), (e), and (i), respectively. The number of lattice points contained in the central maximum is approximately the number of times each repeating unit of the object gets superimposed in the filtered reconstruction image. The numbers in these examples are approximately (b) 17, (f) 79, and (j) 314. (c,g,k) Same as Fig.III.77f with masks of (a), (e), and (i) positioned in the transform plane of the optical diffractometer. This shows what information is allowed to pass the transform plane of the diffractometer and recombine in the reconstruction plane. (Note: only the central 3 by 3 portion of the 11 by 11 array is shown here). (d,h,l) Filtered, reconstruction images of Fig.III.77d. The insets are from the identical region shown in the magnified portion of Fig.III.77d. Notice how the original 50 by 50 array of Fig.III.77d becomes larger in the filtered images.

Fig.III.79. Optical filtering demonstration, Part 3: Very 'distorted' structure. (a) 50 by 50 array of an "imperfect" crystal with some very large defects. (b) Enlarged portion of (a). (c,e,g) Filtered images of (a) obtained using the masks of Fig.III.77a,e,i respectively. (d,f,h) Enlarged views of (c), (e),and (g) from the same region as (b). Notice that the holes in the filter mask must be sufficiently small ($d_a * / a^*$ = 0.1) before the noise resulting from the major defects is averaged out. This also demonstrates how a periodicity can be forced on a structure by the action of the mask in Fourier space.

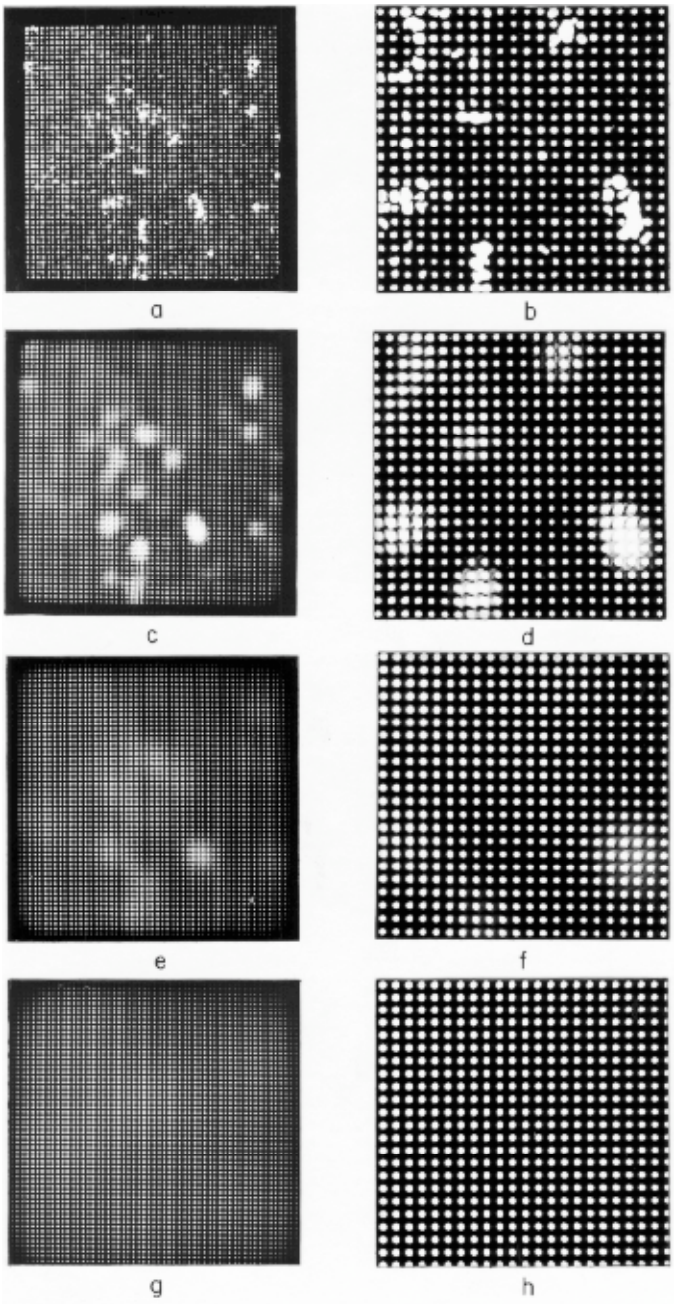


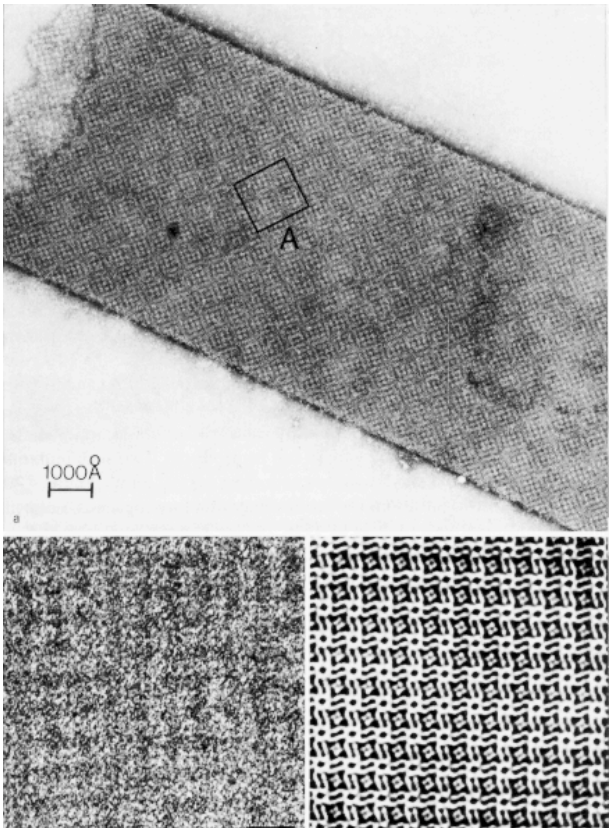


Fig.III.80. Optical filtering of double layer crystal. (a) Image of negatively stained T-layer from *Bacillus brevis*. (b) Enlarged view of area A, consisting of about 10 x 10 unit cells. (c) Optical reconstruction of upper layer of area A. Bar in (b,c) = 200Å. (From Misell, 1978, p.163 adapted from Aebi *et al.* 1973)

### f. Artifacts of optical filtering

Filtered reconstructions often contain undetected, erroneous details as a result of several types of artifacts. Three obvious sources include 1) pattern misindexing resulting in incorrect mask design, 2) incorrect positioning of the mask in the diffraction plane causing spots to be partially or totally blocked, and 3) mispositioned or misshaped mask holes making it impossible to pass all spots through the mask simultaneously. More subtle sources of artifact are indicated in Table 1.II.F of Baker (1981). Some authors contend that ALL reconstructions are, at least in part, erroneous (Berger *et al.*, 1972; Horne and Markham, 1972; Haydon and Scales, 1973; Taylor and Ranniko, 1974).

### g. Comparison with translational photographic-superposition method

The **translational, photographic-superposition method** (also called linear integration: Markham *et al.*, 1964) produces analogous but **not** identical results with those of optical filtering (Figs.III.81-82). The translational parameters (lattice repeat and geometry) are best determined by optical diffraction, not by subjective, trial and error methods (Table 1.IV.B.1.a, Baker, 1981). Despite procedural differences, optical and digital filtering methods produce remarkably similar results (Aebi, *et al.*, 1973; Misell, 1978; Fig. III.83). There are considerable advantages to digital processing (Sec. III.D.3) even though structural details may be reliably represented by either method.

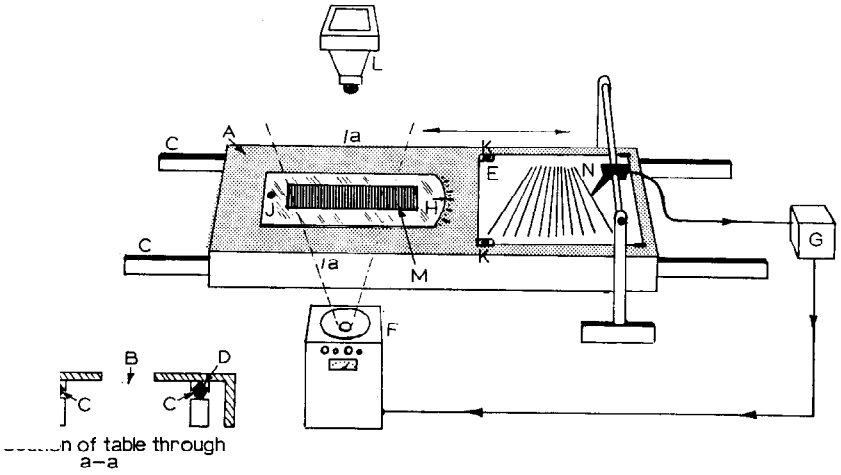


Fig.III.81. The basic arrangement of the linear integrator. (From Horne and Markham, p.421)

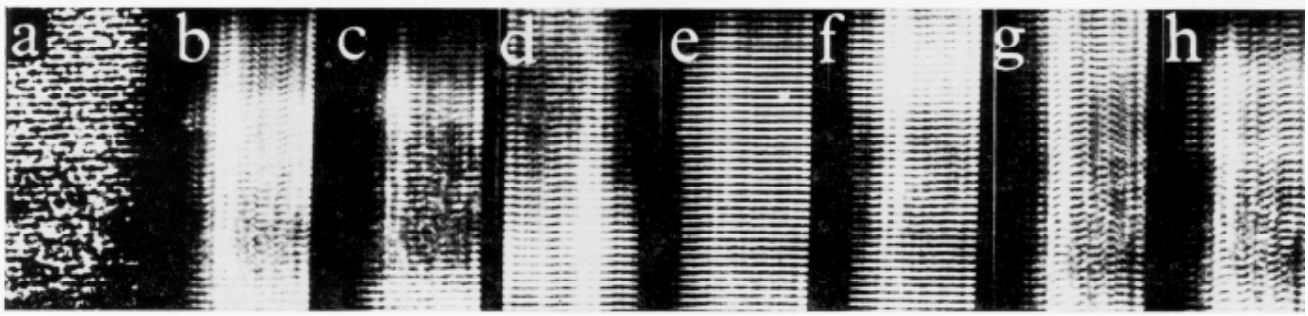


Fig.III.82. Electron micrographs showing repetitive features subjected to integration with the aid of the apparatus shown in Fig.III.76. The lattice spacings in Pt phthalocyanine crystals serve as a good illustration for the application of this technique to provide image reinforcement and accurate measurement. The series of photographs shows the original image (a) after integration at periodicities of b = 1.116, c = 1.142, d = 1.168, e = 1.194, f = 1.220, g = 1.246, and h = 1.272 nm respectively. (From Horne and Markham, p.422)

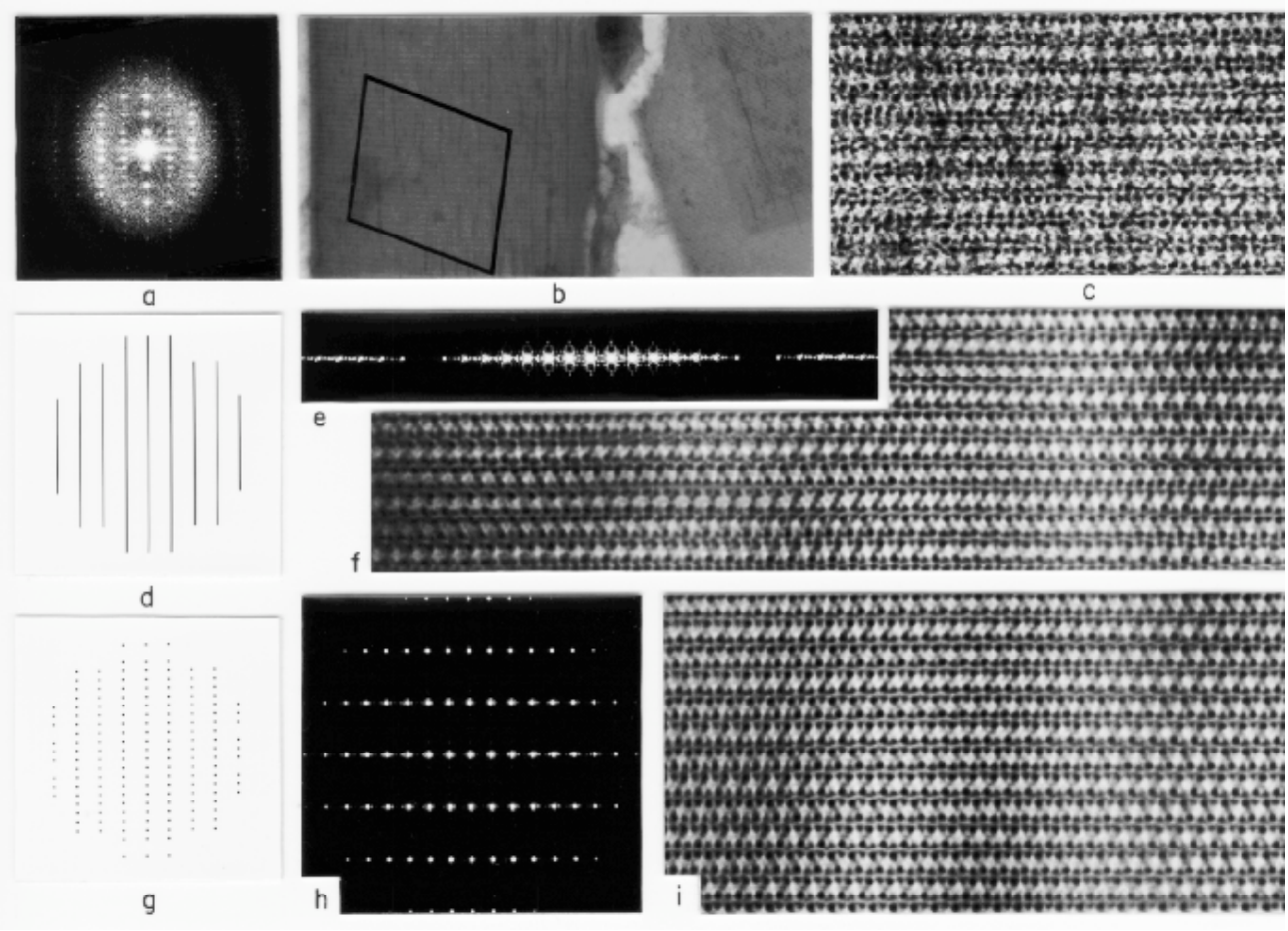


Fig.III.83. Optical filtering demonstration, Part 4. (a) Optical transform of a circular area of (b). (b) Low magnification image of a negatively-stained catalase crystal. The parallelogram shaped area was processed in the filtering experiments (f) and (i). The shape of the window was chosen to minimize diffraction effects on the reconstruction images. (c) Enlarged portion of (b) from the region used for reconstruction. (d) Drawing of mask used for 1D filtering of (b). Magnification is same as in (a). (e) Central portion of the diffraction pattern of (d). (f) Filtered image of (c) obtained with the mask in (d). (g) Drawing of mask used for 2D filtering of (b). Magnification is the same as in (a) and (d). (h) Central portion of the diffraction pattern of (g). (i) Filtered image of (c) obtained with the mask in (g).

Image (f) is obtained by convoluting (c) with the 1D lattice in (e). Note that the weight of each lattice point in (e) and (b) is the square of the superposition weight at that point. This results because the recorded diffraction pattern is the square of the object transform, that is, in (e) and (h) the phase information is lost and only the intensity at each lattice point is recorded. (d)-(f) are an example of an optical analog of the Markham linear superposition method. Notice in (f) that the repeat units are averaged horizontally but not vertically. The extent of averaging is equal to the number of points (15) in the central maximum of the mask transform shown in (e). The number is actually smaller than this because at least half of the superpositions have weights too small to be noticed in the reconstruction (f).

The second filtered image (i) is obtained by convoluting (c) with (b). In (i), therefore, the repeat units are averaged with horizontal as well as vertical neighbors. (f) and (i) are equivalent except that (f) contains vertical components of random or aperiodic noise.

## h. Symbolic mathematical description of optical filtering

The concepts of convolution and sampling (Sec. III.C.6.g, pp. 204-207) provide a fundamental background for understanding the principles of optical reconstruction. Image averaging is simply obtained by convoluting the unfiltered image ($i$) with the Fourier transform of the filter mask ($\boldsymbol{T}(M) = m$). Assuming $\boldsymbol{M}$ is correctly made and positioned in the diffraction plane of the optical diffractometer, then $\boldsymbol{m}$ will cause $i$ to be convoluted with a lattice whose geometry exactly matches that of the crystalline lattice of the specimen imaged. In the following expressions, capital letters are used to designate functions in transform (reciprocal) space, whereas lower case letters denote object (real) space functions.

| IMAGE SPACE | TRANSFORMATION SPACE | RECONSTRUCTION SPACE |
|---|---|---|
| *image* | *T(image)xMASK* | $image * T^{-1}(MASK)$ |
| $i$ | $I \times M$ | $i * m$ |

where $I \times M = I \times [L * H] \times W$

$i * m = i * [I \times h] * w$

$M = [LATTICE * HOLE] \times WINDOW$

$m = [lattice \times hole] * window$

**DEFINITIONS:**

x = multiplication operation.

* = convolution operation.

$T$ = forward Fourier transform operation.

$T^{-1}$ = inverse Fourier transform operation.

$i$ = unfiltered, original micrograph (image).

$I$ = $T(i)$, the forward Fourier transform of $i$.

$M$ = filter *MASK* (a physical entity in an optical filtering experiment).

$m$ = $T^{-1}(M)$, the inverse Fourier transform of *MASK*.

$L$ = *LATTICE* which "exactly" fits the reciprocal lattice of the crystalline object ($i$).

Recall that "*LATTICE*" is **infinite** in extent.

$l$ = $T^{-1}(L)$, the inverse Fourier transform of *LATTICE*. This lattice "exactly" matches the real space crystal lattice **if *LATTICE* is chosen correctly.**

$H$ = *HOLE* in the filtering *MASK* (usually circular ~20-50 $\mu$m diameter).

$h$ = $T^{-1}(H)$, the inverse Fourier transform of *HOLE*. If *HOLE* is circular, $h$ is an Airy function, that is, the Fourier transform of a *HOLE* which is mathematically defined as $J_1(X)/X$ (where $J_1(X)$ is a first order Bessel function).

$W$ = *WINDOW* or boundary which limits the overall extent of the *MASK*.

$w$ = $T^{-1}(W)$, the inverse Fourier transform of *WINDOW*. If the boundary of the *HOLES* in *MASK* is square or rectangular, $w$ is a $\sin(X)/X$ function (a sharp "spike"). If *WINDOW* is circular, $w$ is a $J_1(X)/X$, but note that $w$ is a much sharper function than $h$ because $W$ is larger than $H$ (Law of Reciprocity).

$I \times M$ = filtered diffraction pattern.

$i * m$ = filtered image, or the original image convoluted with the Fourier transform of *MASK*.

## III.D.3. Digital Fourier Analysis of Electron Micrographs

Processing images by digital rather than optical Fourier methods offers several advantages. The main advantages are that **digital methods are quantitative and adaptable.** In addition, 3D reconstruction and rotational filtering are impractical or nearly impossible to achieve with optical techniques. It is also not practical to carry out quantitative analysis and data manipulation on an optical bench. For example, image aberrations such as astigmatism and defocusing, or specimen distortions such as crystal lattice imperfections or curvature in filamentous specimens can be corrected quite easily with digital procedures (Table 1.III.B.6, Baker, 1981). Diffraction amplitudes and phases can be measured and modified, for example, to correct for contrast transfer effects (see Table 1.III.C.3.g, Baker, 1981). Another advantage of digital processing is that separate image reconstructions can be averaged together and a measure of their agreement can be quantified (Table 1.III.B.3.b,c, Baker, 1981). Digital processing offers virtually infinite flexibility in data manipulation**.** For example, in "pseudo-optical filtering", the digital equivalent of optical filtering, filter masks with an infinite variety and combination of hole sizes, shapes, and "transparencies" can be designed.

Computer image processing has replaced the requirement for high-quality, expensive optical systems. Nevertheless, there are **certain disadvantages** such as the necessity for discrete sampling of the data. This produces aliasing artifacts (transform overlap) that can be reduced, although never totally eliminated, by judicious choice of scanning conditions. DeRosier and Moore (1970) define and discuss the aliasing problem inherent to digital image processing.

The initial costs in time and money in setting up a functioning digital system can be prohibitive unless one is genuinely committed to image processing studies. It is fruitless to develop a digital system just to view specimen diffraction patterns. An optical diffractometer is both inexpensive and operates at the speed of light! In addition, the qualitative results of careful optical filtering studies are comparable to those obtained with digital methods (Aebi, *et al.*, 1973; Misell, 1978) despite the small differences resulting from digital aliasing errors (see next section, III.D.3.a). Optical diffraction is the best way to assess the quality of images since it is fast and inexpensive compared to digital methods. Aebi, *et al.* (1973), Misell (1978) and the table in the next section compare the advantages and disadvantages of optical and computer Fourier processing methods. Additional applications and selected examples of digital processing are outlined in Table 1.III.B of Baker (1981).

### a. Comparison of optical and computer image analysis

Despite the obvious differences, optical and digital Fourier processing of electron micrographs are similar in many ways. The advantages and disadvantages of each of these procedures is summarized in the following table:

| OPTICAL | COMPUTER |
|---|---|
| Original micrograph used | Micrograph digitized and "floated" |
| Bench required for diffraction can be simple and inexpensive | Requires fast computer for “interactive” results |
| Formation of diffraction pattern instantaneous | Careful digitization is normally slow and computation of diffraction patterns may take several seconds or longer |
| Filtering operations require high quality (*i.e.* expensive) optics | Computers get more powerful and cheaper every day |
| Accurate filter masks tedious to make | Only limited by quality of software |
| Filtered image recorded photographically | Reconstructed images displayed and photographed using computer graphics devices |
| Quantitative information difficult or nearly impossible to obtain | Essence of computing IS to be quantitative |

| OPTICAL | COMPUTER |
|---|---|
| Amplitudes and phases difficult to manipulate | Infinite control over amplitudes and phases |
| Attenuation of zero-order beam to improve contrast in filtered image (may cause frequency doubling) | Control of contrast simple and straightforward |
| Imposing idealized, non-translational symmetries virtually impossible | Any symmetries (even incorrect) can be easily imposed |
| Correction for lattice distortion virtually impossible | Lattice distortions can be corrected (reinterpolate original image onto perfect lattice) |
| Data (diffraction patterns and filtered images) are continuous (*i.e.* vary smoothly) | Data are discrete (pixels) |
| Fast for screening and selecting best images for additional analysis | Not until CCD technology gets cheap |
| Reconstruction of 3D structure essentially impossible | Procedures rather straightforward with "right" software |
| Impractical to average data from different micrographs | Easy to average data from different micrographs |

## b. Digital processing steps

A typical digital processing procedure includes the following steps:

- Image selection
- Densitometry
- Boxing and floating
- Fourier transformation
- Indexing 2D lattices (for objects with translational symmetry)
- 2D filtering/ 3D reconstruction

*Image selection*

After an initial screening by eye (to discard obvious bad images), micrographs are examined by optical diffraction to select a subset of the "best" images in terms of both optical quality and specimen preservation. These images are then examined by digital processing methods. The optical diffraction pattern quickly reveals the electron optical conditions present when the micrograph was recorded (defocus level, astigmatism, drift, vibration, etc.). Optical diffraction is generally an unsuitable method for selecting images of individual particles with well-preserved symmetry, for example, for digital, rotational filtering. Instead, the rotational power spectrum is computed from the digitized image and analyzed (Sec. III.E.3).

*Densitometry*

The micrograph is digitized on a **scanning densitometer**, a device that converts optical densities on the photographic emulsion to a digital image (a numerical array corresponding to the optical densities at discrete positions in the image). Several types of densitometers are available. The most precise and most expensive are the flatbed type devices (*e.g.* Figs.III.84-86), which digitize the micrograph, laid flat. In rotating-drum densitometers, the micrograph is fixed to a cylindrical surface (drum) and the micrograph is scanned while it is translated along and rotated about the drum axis. A demonstration of the operation of the flatbed type microdensitometer will be given in class. The use of CCD (charge coupled device) cameras for microdensitometry is gaining popularity as they become more affordable.

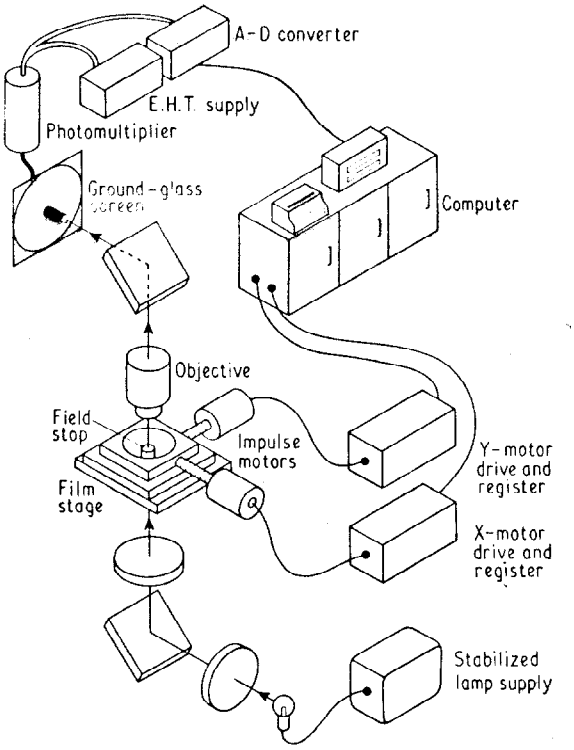


Fig.III.84. Schematic view of the principal parts of the microdensitometer. (From Arndt *et al.*, 1969, p.386)

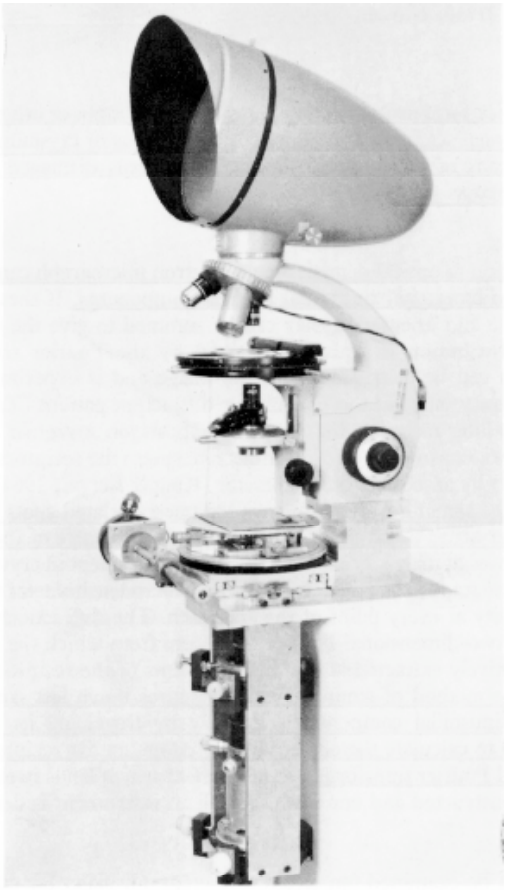

Fig.III.85. Photograph of a combined optical diffractometer and microdensitometer. (From Longley, 1980, p.248)

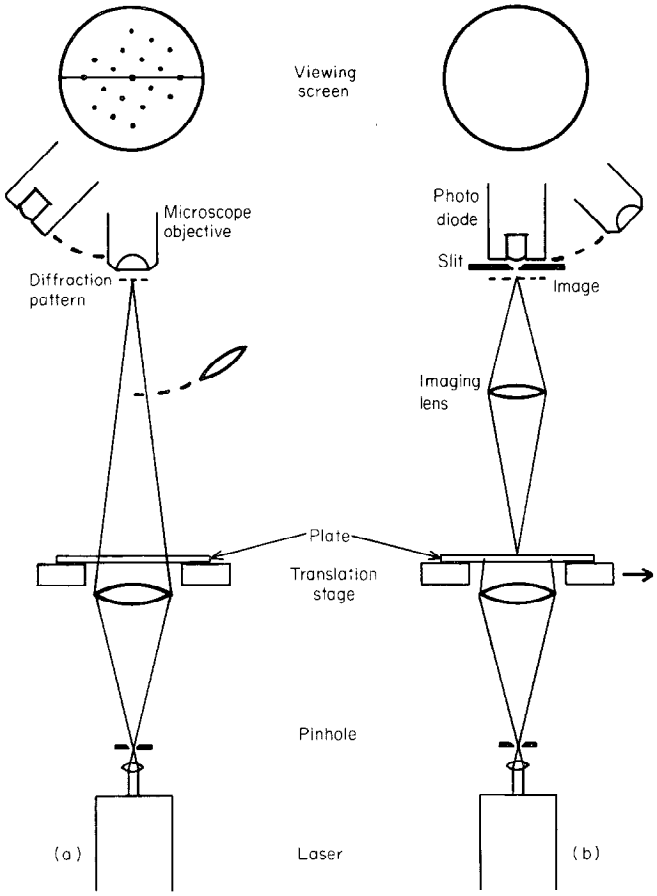


Fig.III.86. Ray diagram: (a) the instrument as a diffractometer; (b) as a microdensitometer. (From Longley, 1980, p.249)

The density value at each point in the digitized image is represented as a **pixel** with intensity ranging between 0 and 255 (an eight-bit number) or 4096 (12-bit number) or even higher in some CCD cameras. The information contained in a single 1024 by 1024 digital image (1,048,576 pixels) is quite staggering: it is roughly equivalent to slightly more than the **entire** contents of the lecture notes (text only) for the combined BIO595R and 595W classes. Note that, at a raster step size of 7 μm (smallest step size on our Zeiss flat-bed densitometer), the area of the micrograph digitized for a 1024 by 1024 array would be ~50 $mm^2$ or only 0.625% (1/160th) of the entire area of a typical 8 x 10 cm micrograph.

Images are scanned at raster settings corresponding to **one-third or less** of the expected pixel resolution in the image to minimize aliasing artifacts (Table 1.III.C.2.c, Baker, 1981; Figs.III.87-88). The equivalent step size (pixel resolution) in the biological specimen depends on the magnification of the micrograph or photograph scanned. For example, if the micrograph was recorded at a magnification of 45,000X and scanned at 14 μm intervals, then each pixel corresponds to 0.311 nm at the specimen. Thus, the **maximum resolution** one can expect to recover from the digitized image is about 0.933 nm (= 3 x 0.311). This assumes the specimen is preserved to *at least* this resolution **and** the electron optical conditions allow recovery of this information. The following table identifies the **maximum pixel resolution** (in nm) recoverable from a digitized image, for images at different magnifications and scanned at different step sizes (those available, for example, on a Zeiss microdensitometer).

**Maximum Pixel Resolution (nm)**

| FEI CM300 MICROGRAPH MAG | ZEISS PHODIS SCAN STEP SIZE (μm) | | | |
|---|---|---|---|---|
| | 7 | 14 | 28 | 56 |
| 13,500 | 0.519 | 1.037 | 2.074 | 4.148 |
| 19,500 | 0.359 | 0.718 | 1.436 | 2.872 |
| 24,000 | 0.292 | 0.583 | 1.167 | 2.333 |
| 33,000 | 0.212 | 0.424 | 0.848 | 1.697 |
| 45,000 | 0.156 | 0.311 | 0.622 | 1.244 |
| 61,000 | 0.115 | 0.230 | 0.459 | 0.918 |

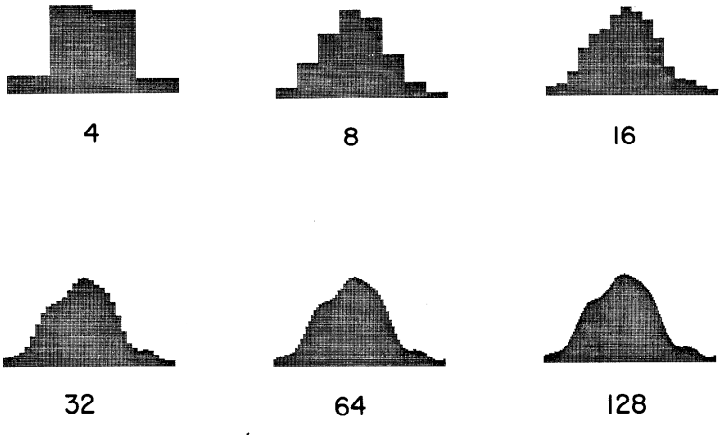


Fig.III.87. Effect of sampling interval on recovery of information. In this example, a sampling interval of 32 appears to be just fine enough to recover the shape of the 1D function without loss of information. At coarser sampling intervals (4-16), the subtler features in the data are lost. In practice, one aims to digitize the data at a fine enough interval to be certain that no information is lost. Thus, using the three-times pixel resolution criteria, in this example one ought to

sample the data 96 (= 3 x 32) or greater to be certain to recover all the information contained in the data.

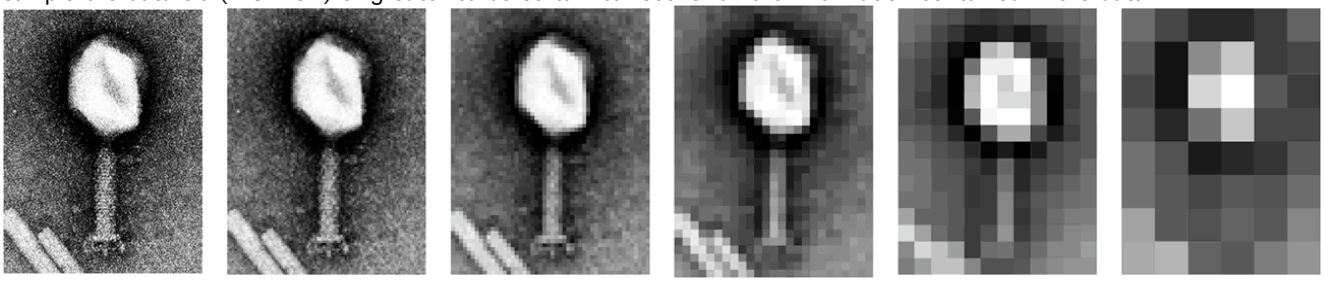

Fig.III.88. Scanned image of negatively stained bacteriophage T4, sampled at different step-sizes. Left to Right: 200, 100, 50, 25, 12, and 6 dpi (dots per inch).

Microdensitometers are computer-controlled devices. They measure optical densities in the micrograph on a square grid (*i.e.* at equal-spaced intervals in *x* and *y* directions: Fig.III.84). The change in intensity of a small beam of light after it passes through the micrograph is measured using a photomultiplier, which converts the analog signal (beam of light) to a digital signal (intensity value typically between 0 and 255). The digitized data can be displayed directly on a raster graphics TV screen or stored on various media (*e.g.* magnetic disk or magnetic tape) for subsequent manipulations. Since digitized images quite often contain significantly large amounts of data (pixels), they are normally stored on magnetic tape when not being processed or analyzed. Several years back, before the days of high capacity 8mm and 4mm tape storage technology, the large (2400'), 1600 bpi (bits per inch), 9-track magnetic tapes only held about 25 1024 by 1024 images (with each pixel stored as a 16 bit value). The higher density (6250 bpi) magnetic tapes could store four times as much data. For those old enough to remember, the double-sided, single-density floppy diskette once used in personal computers could only store 360 Kbytes (here one byte = 16 bits) which is barely sufficient for **one** 512 by 512 image. Modern 4mm and 8mm tape backup technology with up to 12GB (GB = gigabyte) and even larger capacity, means that up to **ten or more thousand** $1024^2$ images can be stored!!! However, this seemingly wonderful capacity has a potential downside: the chores of bookkeeping such massive amounts of data can become a nightmarish problem as well as retrieving such image data.

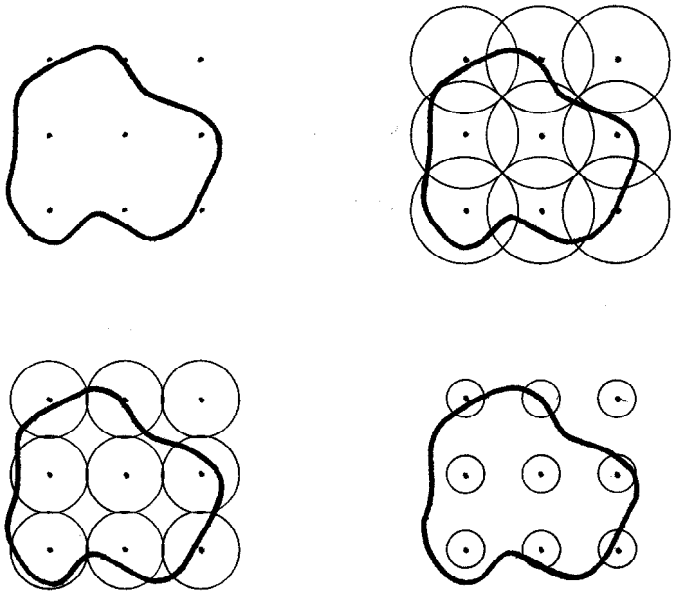

Fig.III.89. Sampling a 2D image on a square lattice. Upper left shows the sampling if it could be performed at discrete points. Lower left shows the usual situation in which the diameter of the illuminating light beam exactly matches the sampling interval. In the upper right panel, the illuminating beam is larger than the raster, which leads to smearing of information because the intensity of the image in neighboring regions gets averaged in with the intensity of the area adjacent to each lattice point. The illuminating beam in the lower right panel is too small, thus only a small fraction of the area defined by the sampling lattice is illuminated about each point. The ideal situation would occur if the image could be illuminated with a square beam, whose dimensions exactly matched the sampling lattice. This is not accomplished in practice.

*Boxing and floating the digital image*

The entire digital image or selected (**boxed or windowed**) areas may be used for subsequent

processing steps. If only a portion of the scanned image is needed, the area of interest is boxed in a manner similar to that used to mask micrographs for optical diffraction and filtering experiments. Thus, areas outside the biological specimen (*e.g.* carbon film or neighboring specimens, etc.) can be selectively removed since these areas mainly contribute noise to the image. Boxing is conveniently performed directly with the digital image displayed on a computer graphics monitor.

Regions of the digital image outside the area of interest are zeroed (equivalent to masking out an area of the micrograph for optical diffraction) and the numerical image is "**floated**" by subtracting the average image intensity around the perimeter of the boxed area from ALL image intensities within the masked area. Floating suppresses intense diffraction spots generated by edges of the masked area. The characteristic "cross" observed in optical diffraction patterns is caused by the strong diffraction that occurs at the edges of the square or rectangular mask where the contrast is much higher compared to that within the windowed portion of the micrograph. As you encounter pictures of diffraction patterns in the literature, make note of the presence or absence of the strong diffraction peaks near the center of the pattern. The presence of a strong spike or other diffraction at the center of the transform indicates that the pattern was generated optically. Alternatively, if the pattern was generated on a computer and still shows strong diffraction spikes or other such effects, this would signify that the image was not floated properly before Fourier transformation.

*Fourier transformation*

Fourier transformation of the numerical array is usually computed by means of Fast-Fourier methods (Table 1.III.C.3.c, Baker, 1981). Often the boxed image is 'padded' to produce a larger image whose dimensions are powers of two (*e.g.* $64^2$, $128^2$, $256^2$, 64x512, etc.). Thus, if the original boxed image was a 55 by 450 pixel array, then this image would be padded AT LEAST out to a 64 by 512 array and then Fourier transformed. Padding just adds pixels with zero intensity to the columns and rows of the boxed image array to make it meet the power of two criteria. This is NOT an essential criteria but it can lead to faster computation of the Fourier transform because some fast-Fourier transform (FFT) computer algorithms are more efficient with images sized this way.

The Fourier transform of an *n* by *m* image results in an *n* by *m* complex array of numbers. Each complex number is a Structure Factor (Sec.III.C.6.f). Each Structure Factor is stored in computer memory either as a structure factor amplitude and phase or as the real (A-part) and imaginary (B-part) parts of the Structure Factor (Sec.III.C.6.f). Diffraction amplitudes and phases may be displayed in a variety of ways, but typically on a computer graphics screen.

*Indexing of two-dimensional lattices*

As has already been emphasized, successful application of image analysis procedures requires correct indexing of the diffraction pattern. For well-ordered, 2D crystalline biological specimens, the diffraction pattern is dominated by a series of discrete spots (Bragg reflections) that lie on a reciprocal lattice. Such patterns are usually fairly easy to index (*i.e.* define the reciprocal lattice parameters and assign Miller indices to each of the spots). Recall that indexing is often already accomplished as a consequence of having inspected an optical diffraction pattern of the specimen image. The indexing of multilayered or two-sided structures (*e.g.* biological aggregates with helical symmetry) can be quite tricky, so care must be used before proceeding to the next step (filtration and reconstruction).

*2D Filtering / 3D Reconstruction (Back-transformation)*

Correct indexing of a diffraction pattern is tantamount to deciding which regions of the Fourier transform are attributed to 'noise' and which regions are attributed to 'signal'. Once the decision is made as to what is signal and what is noise, the computed Fourier transform is 'masked' in a manner completely analogous to the process used to mask the diffraction pattern on an optical bench (Sec.III.D.2). Thus, the amplitudes in the computed Fourier transform are zeroed everywhere except at the reciprocal lattice points. In **pseudo-optical filtering**, the term "points" actually refers to finite regions ("holes" in the "filter mask") centered at the mathematical points of an

ideal reciprocal lattice: these are left as is or may be multiplied by a function which weights highest those transform values lying closest to the ideal lattice. The modified ("filtered") diffraction pattern is mathematically back-transformed to reconstruct an averaged, reconstructed image. **Complete Fourier averaging** (all unit cells are averaged together with equal weight) is accomplished by computing a single Structure Factor amplitude and phase at each of the reciprocal lattice points and reconstructing the structure of a single unit cell by Fourier synthesis (Sec. III.C.6.c, pp.196-198).

Reconstructions may be displayed in a variety of ways. 'Old-timers' (and readers of the original image analysis literature) will recall the use of character over-printing on a line-printer, contour plotting, cathode ray density plotting, film writing, etc. (see Table 1.IV.B of Baker, 1981 for citations of examples). Modern 2D raster graphics devices provide a variety of ways to render such reconstructions in clear, interpretable form.

If the 3D structure of a particle is to be reconstructed, Structure Factor phases and amplitudes must be determined in three dimensions to fill in and generate a complete, 3D Fourier transform. This is accomplished, in the case of a 2D crystal structure, by combining Structure Factor data from several 2D diffraction patterns of independent views of the crystalline specimen. The extent of the 3D transform, and hence ultimate resolution that can be computed, depends both on the number and uniqueness of the specimen images that are included in the data set. Note that, in theory, one could add an 'infinite' number of images to achieve 'infinitely' high resolution, but, in reality, the actual resolution is limited by many other factors (*e.g.* radiation damage to the specimen, specimen distortions, image drift and astigmatism, defocus level, etc.).

The rationale for collecting and combining information from distinct views differs depending on the type (*e.g.* helical, spherical, 2D, 3D, etc.) of specimen being studied (Sec. III.E).

### c. Hardware/Software

Two major disadvantages of digital processing are the expense and complexity of the required hardware (microdensitometer and computer) and software (programs for carrying out the image processing procedures). Most protein crystallography laboratories are equipped with the needed hardware, and often have programs (for example, Fast-Fourier transform, film scanning, and plotting routines) which are easily adapted for most of the basic image processing tasks. Microdensitometers can cost up to $150,000 for the highest precision, flat-bed types. Most multi-user image processing can be performed quite adequately now on computer graphics workstations costing as little as $5,000 or less. The flatbed densitometer has proved to be useful for examining data from unstained specimens studied by low-dose imaging techniques. Here, images recorded at medium-low magnification (10,000-40,000x), containing medium-high resolution details (0.5-2.0 nm), require a small scan raster and aperture (<20 $\mu$m). Also, reflections in electron diffraction patterns (from which diffraction amplitudes are determined from specimens studied by low dose) are usually 20 $\mu$m or smaller in diameter and must be scanned with high precision on a very fine raster (<5 $\mu$m).

Many laboratories engaged in digital processing studies prefer to tailor their own computer software systems since the programs can then be designed to efficiently analyze specimens of particular interest. In this way, results become easier to understand and interpret. If a highly specialized system is not essential, it might be advantageous to acquire a portable, established system developed by others (*e.g.* Table 1.III.c.3.a, Baker, 1981). This can save considerable effort (and frustration) in the development and testing of programs. The main disadvantage of "black-box" systems is the danger of incorrect implementation by untrained users.